ELSEVIER

Journal of Nuclear Materials 305 (2002) 90–96

journal of nuclear materials

www.elsevier.com/locate/jnucmat

# Phase studies in the Rb–Sr–U–O system: characterisation of new phases

Meera Keskar, R. Agarwal, K.D. Singh Mudher *

*Fuel Chemistry Division, Bhabha Atomic Research Centre, Trombay, Mumbai 400 085, India*

Received 17 April 2002; accepted 3 August 2002

**Abstract**

The subsolidus phase relations in the Rb–Sr–U–O system were determined at 900 °C. Two new quaternary phases $Rb_2Sr_2U_4O_{15}$ and $Rb_8Sr_2U_6O_{24}$ in the Rb–Sr–U–O system were synthesized by heating the respective oxides at 900 °C in air. A pseudo-ternary phase diagram of $Rb_2O$–SrO–$UO_3$ was drawn using the new quaternary compounds, and various phase fields were established by X-ray powder diffraction analysis. X-ray powder diffraction (XRD) data of $Rb_2Sr_2U_4O_{15}$ were indexed by a monoclinic system with cell parameters, $a = 0.7875(4)$ nm, $b = 1.3199(4)$ nm, $c = 0.6667(5)$ nm and $\beta = 104.93(8)°$, whereas XRD data of $Rb_8Sr_2U_6O_{24}$ were indexed by a cubic cell with $a = 0.8743(1)$ nm. The structure of $Rb_8Sr_2U_6O_{24}$ was derived from the powder data and structural parameters were refined by the Rietveld profile method.


## 1. Introduction

The knowledge of the interaction of fuel-fission products is important in understanding the behaviour of the fuel during the operation of nuclear reactors. Some of the alkali metals such as rubidium and cesium and alkaline earth metals e.g. strontium and barium have high fission yields, formed during the burn-up of the nuclear fuel. These elements can interact chemically with the $UO_2$ fuel matrix to form ternary and polynary uranium compounds, thus affecting the fuel behaviour. So, the knowledge of phase equilibria and other thermodynamic properties of the alkali and alkaline earth metals is necessary for the advancement of the technology of nuclear energy production.

The alkali metal–uranium–oxygen and alkaline earth metal–uranium–oxygen systems have been investigated extensively, establishing the existence of several uranates and polyuranates depending on conditions like metal-to-uranium ratio, oxygen potential and temperature of reaction. The phase equilibria of alkali metal oxides and their interaction with other oxides relevant to nuclear fuels, fission products and structural materials have been considered in detail in a review by Lindemer et al. [1]. A phase diagram of Na–U–O system at 1000 K was discussed by Kleykamp [2], describing a series of sodium uranates in the system. Several uranates of potassium and rubidium are reported in the literature [3]. The latest revised studies on the partial ternary equilibrium phase diagram of the Rb–U–O system at 1400 K including all the phases investigated in the system were carried out by Iyer et al. [4]. Extensive phase studies and structural information are available on the Cs–U–O system [5]. Solid state chemistry of ternary uranium oxides with alkaline earth metal oxides is reported by Yamashita [6]. In the Sr–U–O system, the ternary SrO–$UO_2$–$O_2$ phase diagram has not been published, whereas the quasi-binary SrO–$UO_2$ phase diagram obtained in air is discussed by Brisi et al. [7] reporting several strontium uranates. However, no studies on the quaternary mixed oxide system involving both alkali metal and alkaline earth metal ions with uranium are reported. In our earlier

* Corresponding author. Tel.: +91-22 5593951; fax: +91-22 5505151.

*E-mail address:* kdsingh@apsara.barc.ernet.in (K.D. Singh Mudher).

0022-3115/02/$ - see front matter 
PII: S0022-3115(02)01156-X

work we have published the preparation and structure of $K_8A_2U_6O_{24}$ compounds (A = Ca, Sr and Ba) [8]. The aim of the present work is to establish the phase relationship in the Rb–Sr–U–O system as a prelude to investigations of a series of alkali metal–alkaline earth metal uranates. The investigations were carried out by preparing various phases of different compositions in the Rb–Sr–U–O system which were characterised by the X-ray powder diffraction (XRD) method.

## 2. Experimental

### 2.1. Sample preparation

$UO_3$, $Rb_2CO_3$ (Aldrich, 99.9%) and $SrCO_3$ (Merck, 99.99%) were used as the starting materials. $UO_3$ was prepared by precipitating a uranyl nitrate (nuclear pure) solution as ammonium diuranate (ADU) with ammonia and decomposing it at 350 °C. The formation of β-$UO_3$ was confirmed by comparing the XRD data with those reported in the literature [9]. $Rb_2CO_3$ and $SrCO_3$ were dried overnight at 200 °C before weighing. As $Rb_2CO_3$ is very hygroscopic, it was weighed in a dry box with a weighing error of 1–2%. Stock solutions were prepared by dissolving $Rb_2CO_3$, $SrCO_3$ and $UO_3$ salts in 1–2 M $HNO_3$ to get molarity of around 0.5 M. The solutions were mixed in different molar ratios of $Rb_2CO_3$, $SrCO_3$ and $UO_3$ for making twenty two equilibrium mixtures listed in Table 1. A few drops of glycerol were added to the mixed solutions which were evaporated to dryness to get homogenised amorphous powder [10]. These powdered mixtures were heated at 900 °C in air, in platinum boats, for 30 h with intermittent grinding and mixing and the products were air quenched.

### 2.2. Instrumental analysis

The XRD data of all the heated products were recorded using graphite-monochromatised Cu $K\alpha_1$ radiation ($\lambda = 0.15406$ nm) on a DIANO X-ray diffractometer at the rate of 1° ($2\theta$) per minute to analyse the formation of various phases. The phases identified in the samples are listed in Table 1 along with their composition. For the structure derivation of one of the phases data collection was done in the range 13–100° ($2\theta$) with step size of 0.02° ($2\theta$) and a counting time of 5 s for each step. The structural parameters were refined using the program DBWS 9411 [11].

## 3. Results and discussions

### 3.1. Phase diagram studies

The three pseudo-binary systems, $Rb_2O$–$UO_3$, SrO–$UO_3$ and $Rb_2O$–SrO were used for establishing the pseudo-ternary phase diagram of the $Rb_2O$–SrO–$UO_3$

Table 1
Phase identification of various compounds in the $Rb_2O$–SrO–$UO_3$ system

| Mixture number | Mole fraction of oxides | | | Phases identified | | |
|---|---|---|---|---|---|---|
| | $x$(SrO) | $x$($Rb_2O$) | $x$($UO_3$) | | | |
| M1 | 0.10 | 0.40 | 0.50 | $Rb_2Sr_2U_4O_{15}$ | $Rb_8Sr_2U_6O_{24}$ | $Rb_2UO_4$ |
| M2 | 0.10 | 0.33 | 0.57 | $Rb_2Sr_2U_4O_{15}$ | $Rb_2U_2O_7$ | $Rb_2UO_4$ |
| M3 | 0.12 | 0.38 | 0.50 | $Rb_2Sr_2U_4O_{15}$ | $Rb_8Sr_2U_6O_{24}$ | $Rb_2UO_4$ |
| M4 | 0.47 | 0.13 | 0.40 | $Rb_8Sr_2U_6O_{24}$ | $Sr_2UO_5$ | – |
| M5 | 0.50 | 0.07 | 0.43 | $Sr_3U_2O_9$ | $Rb_8Sr_2U_6O_{24}$ | $SrUO_4$ |
| M6 | 0.15 | 0.23 | 0.62 | $Rb_2Sr_2U_4O_{15}$ | $Rb_2U_2O_7$ | – |
| M7 | 0.15 | 0.17 | 0.68 | $Rb_2Sr_2U_4O_{15}$ | $Rb_2U_4O_{13}$ | – |
| M8 | 0.22 | 0.25 | 0.53 | $Rb_2Sr_2U_4O_{15}$ | $Rb_8Sr_2U_6O_{24}$ | $SrUO_4$ |
| M9 | 0.55 | 0.15 | 0.30 | $Rb_8Sr_2U_6O_{24}$ | $Sr_3UO_6$ | SrO |
| M10 | 0.40 | 0.05 | 0.55 | $Rb_2Sr_2U_4O_{15}$ | $SrUO_4$ | $Sr_3U_{11}O_{36}$ |
| M11 | 0.15 | 0.10 | 0.75 | $Rb_2Sr_2U_4O_{15}$ | $Rb_2U_7O_{22}$ | $UO_3$ |
| M12 | 0.15 | 0.05 | 0.80 | $Rb_2Sr_2U_4O_{15}$ | $SrU_4O_{13}$ | $UO_3$ |
| M13 | 0.05 | 0.15 | 0.80 | $Rb_2Sr_2U_4O_{15}$ | $Rb_2U_7O_{22}$ | $Rb_2U_4O_{13}$ |
| M14 | 0.05 | 0.35 | 0.60 | $Rb_2Sr_2U_4O_{15}$ | $Rb_2U_2O_7$ | $Rb_2UO_4$ |
| M15 | 0.50 | 0.25 | 0.25 | $Rb_2O$ | $Rb_8Sr_2U_6O_{24}$ | SrO |
| M16 | 0.15 | 0.33 | 0.52 | $Rb_2Sr_2U_4O_{15}$ | $Rb_8Sr_2U_6O_{24}$ | $Rb_2UO_4$ |
| M17 | 0.32 | 0.15 | 0.53 | $Rb_2Sr_2U_4O_{15}$ | $Rb_8Sr_2U_6O_{24}$ | $SrUO_4$ |
| M18 | 0.44 | 0.10 | 0.46 | $Sr_3U_2O_9$ | $Rb_8Sr_2U_6O_{24}$ | $SrUO_4$ |
| M19 | 0.55 | 0.10 | 0.35 | $Sr_3UO_6$ | $Rb_8Sr_2U_6O_{24}$ | $Sr_2UO_5$ |
| M20 | 0.56 | 0.05 | 0.39 | $Sr_2UO_5$ | $Rb_8Sr_2U_6O_{24}$ | $Sr_3U_2O_9$ |
| M21 | 0.15 | 0.20 | 0.65 | $Rb_2Sr_2U_4O_{15}$ | $Rb_2U_2O_7$ | – |
| M22 | 0.17 | 0.17 | 0.66 | $Rb_2Sr_2U_4O_{15}$ | $Rb_2U_4O_{13}$ | – |

system. Those of the $Rb_2O$–$UO_3$ and SrO–$UO_3$ systems have been already investigated. The $Rb_2O$–$UO_3$ pseudo-binary system has four reported compounds [3], $Rb_2U_7O_{22}$, $Rb_2U_4O_{13}$, $Rb_2U_2O_7$, $Rb_2UO_4$, which are made up of $Rb_2O$ and $UO_3$ in the ratios, $(Rb_2O)(UO_3)_7$, $(Rb_2O)(UO_3)_4$, $(Rb_2O)(UO_3)_2$ and $(Rb_2O)(UO_3)$, respectively. The limiting pseudo-binary SrO–$UO_3$ system has six compounds reported by different workers, $Sr_3UO_6$, $Sr_2UO_5$, $Sr_3U_2O_9$, $SrUO_4$, $Sr_3U_{11}O_{36}$, $SrU_4O_{13}$, which are made up of SrO and $UO_3$ in the ratios, $(SrO)_3(UO_3)$, $(SrO)_2(UO_3)$, $(SrO)_3(UO_3)_2$, $(SrO)(UO_3)$, $(SrO)_3(UO_3)_{11}$ and $(SrO)(UO_3)_4$, respectively [7,12,13].

Table 2
The *d*-values of the compounds in the $Rb_2O$–$UO_3$ and SrO–$UO_3$ systems used in this work

| Compound | *d*-values[a] (nm) | | | | | | | | | | Ref. |
|---|---|---|---|---|---|---|---|---|---|---|---|
| $Rb_2U_7O_{22}$ | $0.314_{10}$ | $0.309_{10}$ | $0.364_8$ | $0.342_5$ | $0.728_3$ | $0.401_3$ | $0.981_2$ | $0.585_2$ | $0.249_2$ | $0.202_2$ | [3] |
| $Rb_2U_4O_{13}$ | $0.310_{10}$ | $0.358_5$ | $0.344_5$ | $0.714_4$ | $0.199_4$ | $0.620_2$ | $0.446_2$ | $0.335_2$ | $0.248_2$ | $0.192_2$ | [3] |
| $Rb_2U_2O_7$ | $0.330_{10}$ | $0.693_7$ | $0.347_5$ | $0.289_4$ | $0.200_4$ | $0.343_3$ | $0.290_3$ | $0.232_2$ | $0.193_2$ | $0.174_2$ | [3] |
| $Rb_2UO_4$ | $0.317_{10}$ | $0.308_5$ | $0.416_4$ | $0.694_3$ | $0.218_3$ | $0.180_3$ | $0.185_2$ | $0.159_2$ | $0.154_2$ | $0.282_1$ | [3] |
| $Sr_3UO_6$ | $0.303_{10}$ | $0.298_3$ | $0.502_2$ | $0.428_2$ | $0.309_2$ | $0.214_2$ | $0.177_2$ | $0.173_2$ | $0.256_2$ | $0.214_2$ | [7] |
| $Sr_2UO_5$ | $0.329_{10}$ | $0.313_{10}$ | $0.564_8$ | $0.505_8$ | $0.283_8$ | $0.202_8$ | $0.198_8$ | $0.196_8$ | $0.383_8$ | $0.379_8$ | [7] |
| $Sr_3U_2O_9$ | $0.322_{10}$ | $0.197_4$ | $0.280_4$ | $0.169_4$ | $0.552_3$ | $0.396_3$ | $0.207_3$ | $0.643_2$ | $0.276_2$ | $0.168_2$ | [7] |
| $SrUO_4$ | $0.319_{10}$ | $0.273_5$ | $0.196_5$ | $0.615_4$ | $0.307_4$ | $0.191_4$ | $0.165_4$ | $0.334_3$ | $0.167_3$ | $0.162_3$ | [7] |
| $Sr_3U_{11}O_{36}$ | $0.349_{10}$ | $0.420_9$ | $0.268_8$ | $0.337_6$ | $0.263_5$ | $0.180_4$ | $0.178_3$ | $0.210_3$ | $0.204_2$ | $0.197_2$ | [13] |
| $SrU_4O_{13}$ | $0.349_{10}$ | $0.420_9$ | $0.268_7$ | $0.337_4$ | $0.180_4$ | $0.178_4$ | $0.263_4$ | $0.210_3$ | $0.197_2$ | $0.161_1$ | [12] |
| $Rb_2O$ | $0.317_{10}$ | $0.302_{10}$ | $0.355_5$ | $0.288_5$ | $0.257_5$ | $0.219_5$ | $0.249_4$ | $0.242_4$ | $0.394_4$ | $0.331_4$ | [15] |
| SrO | $0.258_{10}$ | $0.298_9$ | $0.183_8$ | $0.156_5$ | $0.115_3$ | $0.149_3$ | $0.118_2$ | $0.105_2$ | – | – | [6] |
| $UO_3$ | $0.303_{10}$ | $0.307_9$ | $0.358_7$ | $0.340_6$ | $0.194_4$ | $0.478_3$ | $0.250_3$ | $0.247_3$ | $0.192_3$ | $0.190_3$ | [10] |

[a] Ten strongest lines in descending order of intensity (given as subscripts).

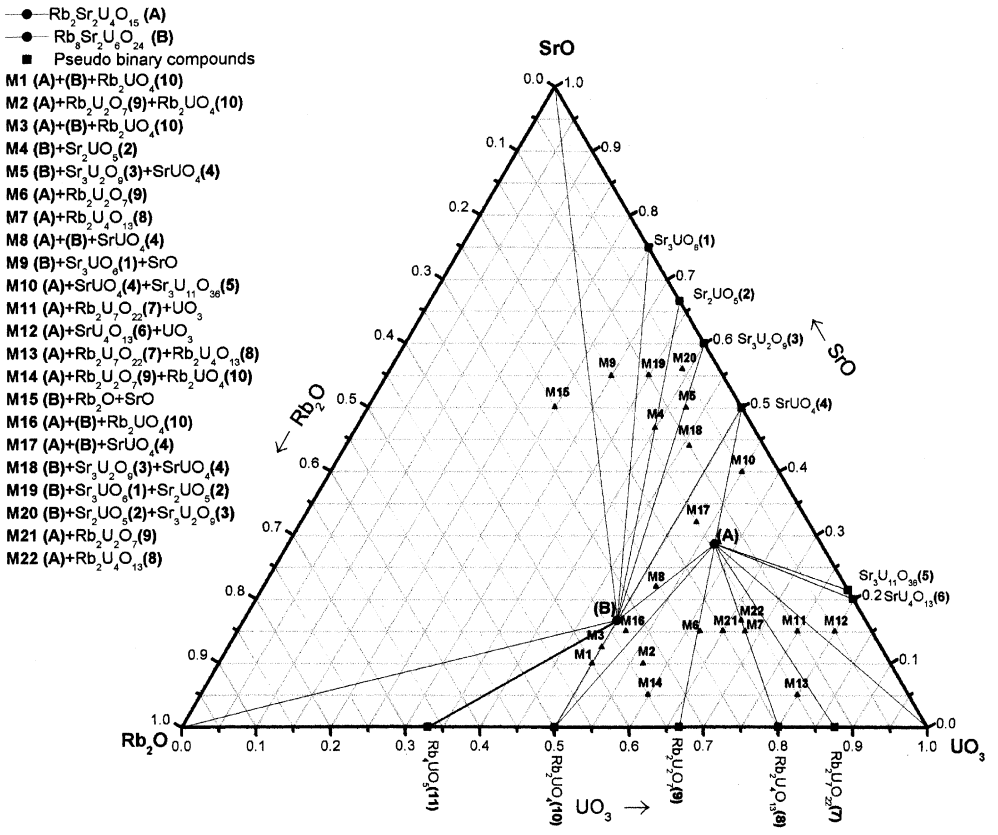


Fig. 1. Isothermal section of the pseudo-ternary phase diagram of the $Rb_2O$–SrO–$UO_3$ system at 900 °C.

Some of these compounds are still not well characterised. In addition, though some phases in both the systems such as $Rb_4UO_5$, $SrU_2O_7$ and $Sr_2U_3O_{11}$ are reported in the literature [6,14], but they are not well characterised and hence not included in the present work. The *d*-values of the ten strongest lines in the decreasing order of intensity of the above mentioned ternary compounds in the $Rb_2O$–$UO_3$ and SrO–$UO_3$ systems, used for the identification of the phases are given in Table 2. No ternary compound is reported in the $Rb_2O$–SrO boundary system. There is no reported solubility of $Rb_2O$, SrO and $UO_3$ in each other or in the compounds formed from them.

A pseudo-ternary phase diagram of $Rb_2O$–SrO–$UO_3$ system shown in Fig. 1 was drawn on the basis of the phase analysis of the samples listed in Table 1 and also using the above mentioned knowledge of the $Rb_2O$–$UO_3$ and SrO–$UO_3$ systems and two new quaternary compounds $Rb_2Sr_2U_4O_{15}$ (A) and $Rb_8Sr_2U_6O_{24}$ (B). Both the quaternary compounds are reported for the first time in this work.

The first novel quaternary phase $Rb_2Sr_2U_4O_{15}$ was obtained by mixing $Rb_2O$, SrO and $UO_3$ in the molar ratio 1:2:4. Heating a mixture of $Rb_2U_4O_{13}$ with 2SrO at 900 °C also formed the compound. XRD patterns of the

Table 3
Indexed powder X-ray diffraction data of $Rb_2Sr_2U_4O_{15}$ of the monoclinic system with $a = 0.7875(4)$ nm, $b = 1.3199(4)$ nm, $c = 0.6667(5)$ nm and $\beta = 104.93(8)°$, $\lambda = 0.15406$ nm

| *h* | *k* | *l* | $d_{obs}$ (nm) | $d_{cal}$ (nm) | $I/I_0$ |
|---|---|---|---|---|---|
| 0 | 1 | 0 | 1.3127 | 1.3199 | 12 |
| 0 | 2 | 0 | 0.6597 | 0.6592 | 100 |
| 1 | 1 | 0 | | 0.6582 | – |
| 1 | 0 | 1 | 0.4392 | 0.4390 | 20 |
| 0 | 4 | 0 | 0.3299 | 0.3296 | 96 |
| 2 | 2 | 0 | | 0.3296 | – |
| 0 | 0 | 2 | 0.3221 | 0.3221 | 4 |
| 0 | 2 | 2 | 0.2894 | 0.2895 | 2 |
| 1 | 4 | 1 | 0.2638 | 0.2638 | 20 |
| −1 | 3 | 2 | | 0.2633 | – |
| −3 | 1 | 1 | 0.2550 | 0.2549 | 5 |
| 3 | 3 | 0 | 0.2197 | 0.2197 | 4 |
| 2 | 0 | 2 | | 0.2195 | – |
| 2 | 5 | 1 | 0.1972 | 0.1972 | 1 |
| −4 | 2 | 1 | 0.1885 | 0.1885 | 18 |
| 4 | 0 | 1 | 0.1709 | 0.1710 | 1 |
| −4 | 0 | 3 | 0.1650 | 0.1650 | 6 |
| 0 | 8 | 0 | | 0.1650 | – |
| 3 | 4 | 2 | 0.1569 | 0.1569 | 1 |
| 0 | 8 | 2 | 0.1468 | 0.1466 | 6 |
| −4 | 6 | 1 | | 0.1467 | – |

Table 4
Indexed powder X-ray diffraction data of $Rb_8Sr_2U_6O_{24}$ ($\lambda = 0.15406$ nm)

| *h* | *k* | *l* | $d_{obs}$ (nm) | $d_{calc}$ (nm) | $I/I_0$ | *h* | *k* | *l* | $d_{obs}$ (nm) | $d_{calc}$ (nm) | $I/I_0$ |
|---|---|---|---|---|---|---|---|---|---|---|---|
| 1 | 1 | 0 | 0.6190 | 0.6184 | 11 | 6 | 2 | 2 | 0.1319 | 0.1318 | 3 |
| 2 | 0 | 0 | 0.4375 | 0.4373 | 27 | 6 | 3 | 1 | 0.1290 | 0.1289 | 2 |
| 2 | 1 | 1 | 0.3568 | 0.3570 | 8 | 4 | 4 | 4 | 0.1262 | 0.1262 | 3 |
| | | | 0.3267[a] | – | 5 | 5 | 4 | 3 | 0.1235 | 0.1236 | 1 |
| 2 | 2 | 0 | 0.3092 | 0.3092 | 100 | 7 | 1 | 0 | | 0.1236 | – |
| 1 | 3 | 0 | 0.2764 | 0.2765 | 3 | 5 | 5 | 0 | | 0.1236 | – |
| 2 | 2 | 2 | 0.2526 | 0.2524 | 3 | 6 | 4 | 0 | 0.1212 | 0.1212 | 1 |
| 2 | 3 | 1 | 0.2336 | 0.2337 | 4 | 6 | 3 | 3 | 0.1191 | 0.1190 | 1 |
| 4 | 0 | 0 | 0.2186 | 0.2186 | 26 | 5 | 5 | 2 | | 0.1190 | – |
| 4 | 1 | 1 | 0.2061 | 0.2061 | 13 | 7 | 2 | 1 | | 0.1190 | – |
| 3 | 3 | 0 | | 0.2061 | – | 6 | 4 | 2 | 0.1169 | 0.1168 | 7 |
| 0 | 4 | 2 | 0.1955 | 0.1955 | 7 | 7 | 3 | 0 | 0.1147 | 0.1148 | 1 |
| 3 | 3 | 2 | 0.1864 | 0.1864 | 5 | 6 | 5 | 1 | 0.1111 | 0.1110 | 1 |
| 4 | 2 | 2 | 0.1785 | 0.1785 | 23 | 7 | 3 | 2 | | 0.1110 | – |
| 5 | 1 | 0 | 0.1715 | 0.1715 | 10 | 8 | 0 | 0 | 0.1093 | 0.1093 | 2 |
| 4 | 3 | 1 | | 0.1715 | – | 7 | 4 | 1 | | 0.1076 | 1 |
| 5 | 2 | 1 | 0.1596 | 0.1596 | 2 | 5 | 5 | 4 | 0.1075 | 0.1076 | – |
| 4 | 4 | 0 | 0.1546 | 0.1546 | 9 | 8 | 1 | 1 | | 0.1076 | – |
| 5 | 3 | 0 | 0.1498 | 0.1499 | 2 | 8 | 2 | 0 | 0.1060 | 0.1060 | 2 |
| 4 | 3 | 3 | | 0.1499 | – | 6 | 4 | 4 | | 0.1060 | – |
| 6 | 0 | 0 | 0.1457 | 0.1458 | 3 | 6 | 5 | 3 | 0.1045 | 0.1045 | 1 |
| 4 | 4 | 2 | | 0.1458 | – | 8 | 2 | 2 | 0.1031 | 0.1030 | 5 |
| 6 | 1 | 1 | 0.1418 | 0.1418 | 2 | 0 | 6 | 6 | | 0.1030 | – |
| 5 | 3 | 2 | | 0.1418 | – | 8 | 3 | 1 | 0.1016 | 0.1016 | 1 |
| 6 | 2 | 0 | 0.1383 | 0.1383 | 9 | 3 | 4 | 7 | | 0.1016 | – |
| 5 | 4 | 1 | 0.1349 | 0.1349 | 1 | | | | | | |

[a] The unindexed line belongs to the $Rb_2U_2O_7$ phase.

products obtained by both the methods were exactly the same, thus confirming the formation of $Rb_2Sr_2U_4O_{15}$ by different routes. The XRD data of the compound were indexed by a monoclinic system with the cell parameters $a = 0.7875(4)$ nm, $b = 1.3199(4)$ nm, $c = 0.6667(5)$ nm and $\beta = 104.93(8)°$. The indexed XRD data of $Rb_2Sr_2U_4O_{15}$ are given in Table 3. The second new phase, $Rb_8Sr_2U_6O_{24}$ was obtained by heating a mixture of $Rb_2O$, SrO and $UO_3$ in 4:2:6 molar ratios, respectively. The XRD data of the compound were indexed by a cubic cell with $a = 0.8743(1)$ nm. The indexed X-ray diffraction data of the $Rb_8Sr_2U_6O_{24}$ powder are given in Table 4.

The compositions investigated by XRD analysis to establish the coexisting phases are shown as points, and the respective stable phases are also indicated in Fig. 1. Phase boundaries are drawn on the basis of the reported ternary compounds and the newly detected quaternary compounds. Phase analysis of most of these compositions confirmed the expected phase boundaries. But as can be seen in Fig. 1, the sample number, M21, with an overall composition $(Rb_2O)_{0.2}(SrO)_{0.15}(UO_3)_{0.65}$, is expected to contain three phases: $Rb_2Sr_2U_4O_{15}$, $Rb_2U_2O_7$ and $Rb_2U_4O_{13}$. But XRD analysis of this equilibrium mixture showed the presence of only two phases: $Rb_2Sr_2U_4O_{15}$ and $Rb_2U_2O_7$. According to the mass balance, this equilibrium mixture should be composed of 52.5% $Rb_2Sr_2U_4O_{15}$, 25% $Rb_2U_2O_7$ and 22.5% $Rb_2U_4O_{13}$ or a ratio of $Rb_2U_4O_{13}/(Rb_2U_4O_{13} + Rb_2Sr_2U_4O_{15}) = 0.32$, but the absence of $Rb_2U_4O_{13}$ in the mixture may be due to its limited solubility in the quaternary compound $Rb_2Sr_2U_4O_{15}$. On the other hand, the samples no. M7 and M22 clearly show the presence of the compounds, $Rb_2Sr_2U_4O_{15}$ and $Rb_2U_4O_{13}$. On the basis of the mass balance, M7 should contain 52% $Rb_2Sr_2U_4O_{15}$ and 48% $Rb_2U_4O_{13}$, whereas, M22 should contain 58% $Rb_2Sr_2U_4O_{15}$ and 42% $Rb_2U_4O_{13}$ of each of these compounds. In both the samples, the fraction of $Rb_2U_4O_{13}$ is considerably higher than that in M21. Therefore, it may be possible that the compound $Rb_2U_4O_{13}$ is soluble in $Rb_2Sr_2U_4O_{15}$ (A) when the ratio $Rb_2U_4O_{13}/(Rb_2U_4O_{13} + Rb_2Sr_2U_4O_{15}) \leqslant 0.32$. The X-ray lines of the compound $Rb_2U_4O_{13}$ were very clearly observed in the X-ray pattern of M22. This indicates that the compound, $Rb_2U_4O_{13}$ had precipitated out from the saturated solid solution of $Rb_2U_4O_{13}$ in the quaternary compound $Rb_2Sr_2U_4O_{15}$. The *d*-values of the stronger intensity (0.658, 0.3295 and 0.4392 nm) of the pure compound, $Rb_2Sr_2U_4O_{15}$, were found to shift to higher *d* values for the same compound in M7, M21 and M22, which may be due to the lattice expansion of $Rb_2Sr_2U_4O_{15}$.

Further work needs to be carried out to determine exact solubility limits of $Rb_2U_4O_{13}$ in the quaternary compound $Rb_2Sr_2U_4O_{15}$ and to define the effect of composition on the lattice parameters.

Table 5
Rietveld refinement details for $Rb_8Sr_2U_6O_{24}$

| | |
|---|---|
| Radiation | $CuK_{\alpha_1}$ $\lambda = 0.15406$ nm |
| Space group | Im3m |
| $a$ (nm) | 0.8743(1) |
| $V$ ($nm^3$) | 0.668 |
| $D_{calc}$ ($g\,cm^{-3}$) | 6.64 |
| $Z$ | 1 |
| $R_p$ (%)[a] | 8.99 |
| $R_{wp}$ (%)[b] | 12.12 |
| $R_{exp}$ (%)[c] | 10.52 |

[a] $R_p = 100 \times \Sigma|y_{obs} - y_{cal}|/\Sigma|y_{obs}|$.
[b] $R_{wp} = 100 \times \{[\Sigma w(y_{obs} - y_{cal})^2]/[\Sigma w y_{obs})^2]\}^{1/2}$.
[c] $R_{exp} = 100 \times \{(N - P + C)/[\Sigma w(y_{obs})^2\}]^{1/2}$.

### 3.2. Structural studies

The structure of $Rb_8Sr_2U_6O_{24}$ was derived from the space group Im3m (no. 229) by Rietveld profile analysis of the X-ray powder data, based on the atomic parameters of the isostructural $K_8Sr_2U_6O_{24}$ [8]. The structural parameters of $Rb_8Sr_2U_6O_{24}$ (atomic parameter $x$ of O1

Table 6
Atomic parameters and interatomic distances in $Rb_8Sr_2U_6O_{24}$ values in the parentheses correspond to estimated standard deviations

| Atom | Site | $x$ | $y$ | $z$ | $B_{iso}$ ($nm^2$) |
|---|---|---|---|---|---|
| U | 6b | 0.0 | 0.5 | 0.5 | 0.005 |
| Sr | 2a | 0.0 | 0.0 | 0.0 | 0.008 |
| Rb | 8c | 0.25 | 0.25 | 0.25 | 0.007 |
| O1 | 12e | 0.287(2) | 0.0 | 0.0 | 0.015 |
| O2 | 12d | 0.25 | 0.0 | 0.5 | 0.013 |

*Interatomic distances (nm)*

| | |
|---|---|
| U–O1 2× | 0.186(2) |
| U–O2 4× | 0.2185(1) |
| Sr–Ol 6× | 0.251(2) |
| Rb–Ol 6× | 0.3108(3) |
| Rb–O2 6× | 0.3091(1) |

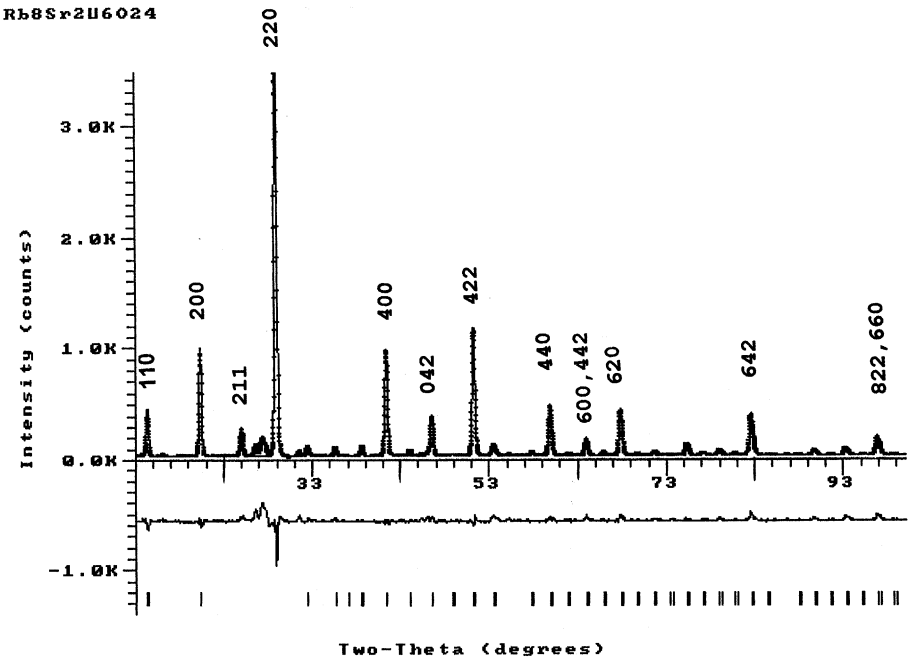


Fig. 2. Rietveld plot of observed and calculated diffraction patterns of $Rb_8Sr_2U_6O_{24}$. The difference plot is shown by the lower trace on the same scale.

and overall thermal parameters of all atoms) were refined, modeling individual diffraction profiles on pseudo-Voigt function. The refinement of the appropriate atomic parameters and profile parameters resulted in agreement factors given in Table 5. The derived atomic parameters of $Rb_8Sr_2U_6O_{24}$ and the relevant bond lengths between different atoms are listed in Table 6. The observed and calculated diffraction patterns of $Rb_8Sr_2U_6O_{24}$ and their difference pattern are shown in Fig. 2. The indices of the intense lines are shown in the figure, pointing to their position.

A two-dimension structure of $Rb_8Sr_2U_6O_{24}$ is shown in the Fig. 3. In the structure all the uranium atoms are present as uranyl ion (U–O1) with four more oxygen atoms O2 in the equatorial plane forming octahedral coordination at distances given in Table 6. Six oxygen atoms O1 at equal distances forming regular octahedral geometry around the metal atom also surround Sr atoms. The structure is made of chains of uranium octahedra (dark) on one side and chains of alternating uranium and Sr octahedra (light) on the other side. The structure can be derived from the perovskite $RbUO_3$ where 1/4 of the U(V) atoms are substituted by $Sr^{2+}$ and thereby forming uranyl octahedra and leading to near doubling of the unit cell of $RbUO_3$ ($a = 0.4327$ nm). Each uranium octahedron is connected to four other uranium octahedra at the corners by four oxygen atoms O2 and to two octahedra around Sr atoms through oxygen atoms of the uranyl group. In this way, the regular

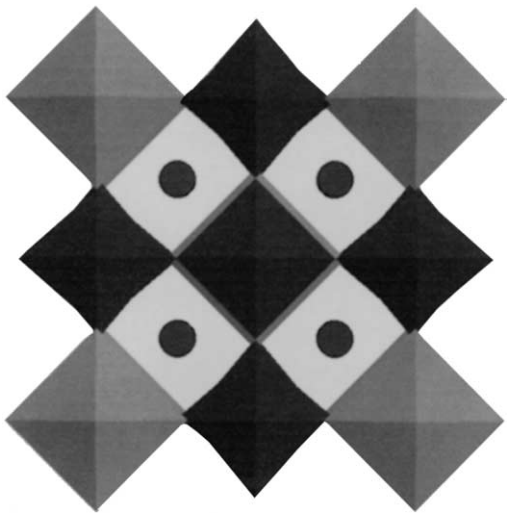

Fig. 3. Two-dimension structure of $Rb_8Sr_2U_6O_{24}$, showing uranium octahedra (dark) and strontium octahedra (light). The position of rubidium atoms are shown as circles in the voids.

octahedra around Sr are also connected at six corners to six uranium octahedra by the oxygen atoms of the uranyl groups. Each rubidium atom located in the voids in Fig. 3, is surrounded by six oxygen atoms O1 and six oxygen atoms O2 at the edges within a cube forming a twelve-coordination geometry at distances ranging from 0.3091 to 0.3108 nm (Table 6).

Attempts to solve the structure of $Rb_2Sr_2U_4O_{15}$ from the powder data were not successful.

## 4. Summary

Two new quaternary phases $Rb_2Sr_2U_4O_{15}$ and $Rb_8Sr_2U_6O_{24}$ in the Rb–Sr–U–O system were prepared and characterised by the powder XRD method. Based on these two new phases, a quasi-ternary phase diagram of $Rb_2O$–SrO–$UO_3$ system has been drawn.

## Acknowledgements

The authors are thankful to Dr V. Venugopal, Head, Fuel Chemistry Division and Shri Rajendra Prasad, Head, Fuel Development Chemistry Section, for their keen interest in this work.

## References

[1] T.B. Lindemer, T.M. Besmann, C.E. Johnson, J. Nucl. Mater. 100 (1981) 178.
[2] H. Kleykamp, Forschungszentrum Karlsruhe Report KFK 4701, 1990.
[3] A.B. Van Egmond, E.H.P. Cordfunke, J. Inorg. Nucl. Chem. 38 (1976) 2245.
[4] V.S. Iyer, K. Jayanti, S.K. Sali, S. Sampath, V. Venugopal, J. Alloys Compd. 235 (1996) 1.
[5] E.H.P. Cordfunke, A.B. Van Egmond, G. Van Voorst, J. Inorg. Nucl. Chem. 37 (1975) 1433.
[6] T. Yamashita, JAERI, Report 1310, 1988.
[7] C. Brisi, M. Montorsi, G.A. Burlando, Rev. Int. Hautes Temp. Refract. 8 (1971) 37.
[8] K.D. Singh Mudher, M. Keskar, Mater. Res. Bull. 35 (2000) 33.
[9] S.R. Daharwadkar, M.D. Karkhanawala, J. Ind. Chem. Soc. 45 (1968) 490.
[10] K.T. Pillai, R.V. Kamat, V.N. Vaidya, D.D. Sood, Mater. Chem. Phys. 44 (1996) 255.
[11] R.A. Young, A. Sakthivel, T.S. Moss, C.O. Paivaa-Santos, program DBWS 9411, Georgia Institute of Technology, Atlanta, GA, 1994.
[12] E.H.P. Cordfunke, B.O. Loopstra, J. Inorg. Nucl. Chem. 29 (1967) 51.
[13] Van Vlaanderen, Neatherlands Energy Research Foundation, Petten, private communication, 1993.
[14] S.K. Sali, PhD thesis, University of Mumbai, 1997.
[15] PDF No. 27-545, International Centre for Diffraction Data, Newtown Square, PA, USA.